Stability and reactivity of C_{60} studied by all-electron mixed-basis molecular-dynamics simulations at finite temperatures

K. Ohno, Y. Maruyama, and Y. Kawazoe
Institute for Materials Research, Tohoku University, Sendai 980-77, Japan
(Received 21 September 1995)

Carrying out *ab initio* molecular-dynamics simulations with an all-electron mixed-basis approach at constant temperatures including Fermi distribution of electronic states, we found that ideal C_{60} with I_h symmetry is selectively regained from a $C_{58}+C_2$ reaction; ideal C_{60} and its C_{2v} isomer become unstable, respectively, at about 4500 and 1500 K; and the deformation observed in a reaction with C_2 at 1000 K is bigger in the C_{2v} isomer than in ideal C_{60}.

I. INTRODUCTION

Recently, C_{60} and higher fullerenes have attracted considerable interests,[1–13] since they are unbelievably stable and have specific cage structures. By using the electric arc discharge technique with controlled atmosphere, C_{60} can be produced with relatively high percentage.[2] As well as other fullerenes, C_{60} satisfies the isolated pentagon rule (IPR),[3] stating that more than two pentagons are not fused on the cage surface. The reason why only structures obeying the IPR are produced during the formation process is nontrivial.[4]

So far, several plausible ideas[5–9] have been proposed to explain the mechanism of the cage structure formation and the selectivity of special isomers. The possibility of spontaneous change of the cage structures during the formation has been discussed in the context of Stone-Walles transformation[4,10] or C_2-loss process.[10,11] (Theoretical studies have indicated that a C_2 loss requires at least 7 eV,[10] if the electronic ground state is assumed.) Meanwhile, classical molecular dynamics[6,11,12] and tight-binding[13,14] simulations have been performed to understand the formation and reaction processes of C_{60}. The obtained results, however, depend strongly on the initial condition, and potential parameters. Moreover, all these theoretical treatments assumed just 60 carbon atoms to form C_{60} cage under suitable temperature control *only for the atomic movements*.

Ab initio molecular dynamics[15–17] and related simulated annealing technique,[16] which do not use any conventional matrix-diagonalization method, are known to be quite efficient with respect to both memory size and CPU time. So far, such simulations have, however, been restricted for fullerenes only to finding the optimized structures of assumed icosahedral cage and small vibrations around them.[18–21]

In this paper, we perform *ab initio* molecular-dynamics simulations with an all-electron mixed-basis approach at constant temperatures including also Fermi distribution of electronic states to study stability and reactivity of C_{60} fullerene. Here we confine ourselves to the following elementary processes: (A) Stability of C_{60}, (B) reproducibility of C_{60} from $C_{58}+C_2$ reaction, (C) reactivity of C_{60} with C_2 (or C_3).

In these simulations, we consider not only an ideal C_{60} with I_h symmetry but also its isomer with C_{2v} symmetry which has two fused pentagons in each side of one hexagon-hexagon bond (hereafter we call this 6/6 bond), and is constructed by 90° rotation of the 6/6 bond in ideal C_{60}.[4,22]

II. METHODOLOGY

Now we take for granted the Born-Oppenheimer (BO) adiabatic approximation, and consider the grand canonical ensemble for the electronic states, where both the temperature and the chemical potential are fixed. For equilibrium system, it is natural for the electronic states to maintain the same temperature as assumed for the atomic dynamics. It will be shown that this effect is really important in the formation process. We adopt the density functional formalism extended to the grand canonical ensemble by Mermin.[23] (In a plasma state at extremely high temperatures, an alternative approach was proposed quite recently.[17]) We then use the corresponding local density approximation due to Gunnarsson and Lundqvist.[24] For the exchange-correlation function, $F^{\mathrm{xc}}[\rho]$, we utilize the $X\alpha$ method with $\alpha=0.7$. Within this formalism, the charge density is given by

$$\rho(\mathbf{r})=2\sum_i \frac{\psi_i^*(\mathbf{r})\psi_i(\mathbf{r})}{e^{(\epsilon_i-\mu)/k_BT}+1}, \tag{1}$$

where the prefactor 2 means the spin duplicity at each level. The chemical potential μ is determined by

$$2\sum_i \frac{1}{e^{(\epsilon_i-\mu)/k_BT}+1}=N, \tag{2}$$

where N is the total number of electrons in the system. ϵ_i and $\psi_i(\mathbf{r})$ are the eigenvalue and eigenfunction of a one-particle Hamiltonian H

$$H=-\frac{\hbar^2}{2m}\nabla^2+e^2\int\frac{\rho(\mathbf{r}')}{|\mathbf{r}-\mathbf{r}'|}-\sum_n\frac{Ze^2}{|\mathbf{r}-\mathbf{R}_n|}+v^{\mathrm{xc}}(\mathbf{r}), \tag{3}$$

where R_n denotes the position of the nth atom, Z the nucleus charge of carbon atom, and $v^{\mathrm{xc}}(\mathbf{r})=\delta F^{\mathrm{xc}}[\rho]/\delta\rho(\mathbf{r})$.

In the all-electron mixed-basis approach, wave functions are expanded by not only plane waves (PW's), but also Slater-type atomic orbitals (STO's).[21] This method has the following advantages: (1) reduction of the number of plane

waves, (2) account of core electrons, (3) no usage of pseudopotential, (4) analytic evaluation of intra-atomic forces and a part of potential matrix elements (interatomic forces and matrix elements of aspherical part of the potential are evaluated numerically), (5) reduction of both memory and CPU time. Note that the pseudopotential approach requires a large number of plane waves, typically 100 000,[25] even for a single C_{60}. (Our method can reproduce fairly well the result of Ref. 25 in the C_{60} crystal with much smaller number of plane waves.[26])

To achieve convergence of electronic states and orthogonalize different electronic levels, we adopt Gram-Schmidt orthogonalization and Payne algorithm,[16] which are commonly used as a usual steepest-descent (SD) algorithm. Moreover, since basis functions are not mutually diagonal in a mixed-basis approach, we start from the modified equation, which guarantees the orthogonality;

$$\mu S\dot{\Psi}_i = -(H - \Psi_i^\dagger H \Psi_i S)\Psi_i , \tag{4}$$

where μ denotes the friction constant for updating electron wave functions Ψ_i, H $(=\langle k|H|l\rangle)$ the Hamiltonian of the electrons, and E the total energy of the system.

The distinction of the present equations of the mixed-basis approach from those of the original PW approach[15–19] is the presence of the overlap matrix S $(=\langle k|l\rangle)$ in Eq. (4), which is due to the fact that the bases are not mutually orthogonal. Introducing the lower half triangular matrix U, which satisfies $S=UU^\dagger$, and writing $U^\dagger\Psi_i=\Phi_i$ and $H'=U^{-1}HU^{\dagger-1}$, we have

$$\mu\dot{\Phi}_i = -(H' - \Phi_i^\dagger H' \Phi_i)\Phi_i . \tag{5}$$

Once we adopt this representation, the main algorithm of updating the wave function Φ_i is the same as the original PW approach.

Five STO's $(1s,2s,2p_x,2p_y,2p_z)$ being located at each atomic site, and 2969 plane waves are adopted as a basis set. The exponential damping factors are chosen to be rather narrow, $\alpha=1/0.18$ a.u.$^{-1}$ (for $1s$) and $\beta=\gamma=1/0.24$ a.u.$^{-1}$ (for $2s,2p$), in order to avoid overlaps between neighboring atoms. Matrix elements and forces associated with STO's are evaluated analytically as far as possible. We use a supercell approximation; a unit cell is divided into $64\times64\times64$ meshes, where 2.7 meshes in length correspond to 1 a.u. $=0.529$ Å. For the computation, we used HITAC S-3800/380 supercomputer (24 GFLOPS) at our Institute with parallel coding. Each SD iteration step took about 20 s, and the present code requires 370 MB in main memory. We adopt 8 a.u.$=0.2$ fs as the basis time step Δt for simulation (A), and 4 a.u.$=0.1$ fs for simulations (B) and (C).

For each simulation, we first fix atomic positions until the electronic states well converge to the BO surface. Atomic dynamics are governed by classical mechanics with the Hellmann-Feynman force at constant temperature by usual velocity rescaling technique. We perform typically 6 SD iterations of electronic states before each update of atomic positions, and one velocity rescaling in every 10 atomic movements. At each SD step, we make new electronic charge density by mixing 50% with the density at the last step in order to stabilize the convergence.

III. RESULT

Let us start by showing the results of the stability simulation (A). We adopted the Fermi distribution, Eq. (1), for the electronic states, and found that an ideal C_{60} and its C_{2v} isomer are unstable, respectively, at 5000 and at 2000 K; breathing modes are excited and finally fragmentations occur, after ca. 300 fs. We confirmed that they (I_h and C_{2v} isomers) are stable, respectively, at 4000 and 1000 K. These results were nontrivial, because, if we assumed the ground state for the electronic states, we observed that these molecules were stable at least up to 10 000 K. The fragmentation temperature of the ideal C_{60} observed in the present simulation is somewhat smaller than 5600 K obtained by the tight-binding study.[13] The electron excitation is of course negligible at low temperatures but becomes important at higher temperatures where $k_BT\sim E_g$ (highest occupied molecular orbital–lowest unoccupied molecular orbital gap energy). Since 10 000 K corresponds to ~1 eV, electron excitation is quite important at these temperatures. Our results explicitly show that the fragmentation is not only due to the excitation of strong atomic vibrations but also due to the weakened interatomic potential caused from electronic excitations at finite temperatures.

We also investigated the optimal structure and vibrational frequencies of C_{60} at 0 K by performing 20 SD iterations per each update of atomic positions. The obtained optimal bond lengths are 1.43 ± 0.02 and 1.46 ± 0.02 Å, respectively, for double bonds and single bonds. The values are not singly peaked but rather scattered because of the usage of the supercell approximation and the shortage of the number of plane waves. But, these data are not very different from the experimental values, 1.397 and 1.455 Å. On the other hand, to estimate vibrational frequencies of the breathing modes (A_g modes) and the rotational modes of hexagonal rings (H_g modes) from our result, we investigated time sweeps of the radius of each atom from the center and the angle of each hexagon from fixed (z) direction. Then, Fourier transforming the corresponding velocities during 500–1900 steps (we omitted data at the first 500 steps in order to avoid initial relaxations), we obtained rough vibration spectra. For A_g modes, we observed several strong peaks between 200 and 500 cm^{-1}, and a few weaker peaks between 600 and 1300 cm^{-1}, while, for H_g modes, we observed many strong peaks between 200 and 1100 cm^{-1}, and several weaker peaks between 1300 and 1800 cm^{-1}. These data are comparable to the previous studies.[19,20]

In the reproducibility simulation (B), we started from C_{58}, which was made from ideal C_{60} by removing two carbon atoms sharing one double bond. After 100 steps for relaxing the initial structure, we injected C_2 dimer from vertical direction toward the C_2 hole of the C_{58} cage; see Fig. 1. In this and all the following figures, we draw bonds only if the bond length is smaller than 1.6 Å. After 400 fs, we found that the incident C_2 is absorbed to reproduce almost an ideal C_{60}, i.e., *not* a C_{2v} isomer of C_{60} that could be generated by 90° rotation of the adsorbed C_2. Hence, IPR is proved in this process of the C_{60} formation. We found, however, that small distortion, i.e., asphericity, around the absorption site still remained after 400 fs. The radius difference was about 0.3 Å. After a sufficient time, this asphericity would experi-

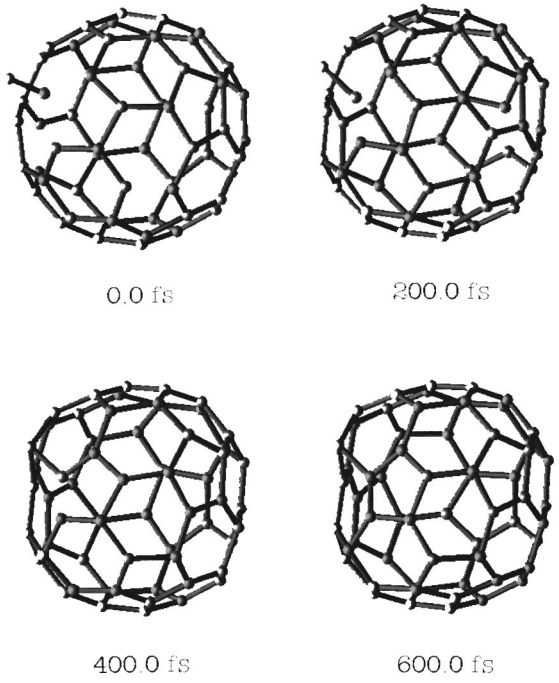

FIG. 1. Snapshots of $C_{58}+C_2$ reaction at 0, 200, 400, and 600 fs. In this simulation, almost ideal C_{60} was retrieved after 400 fs.

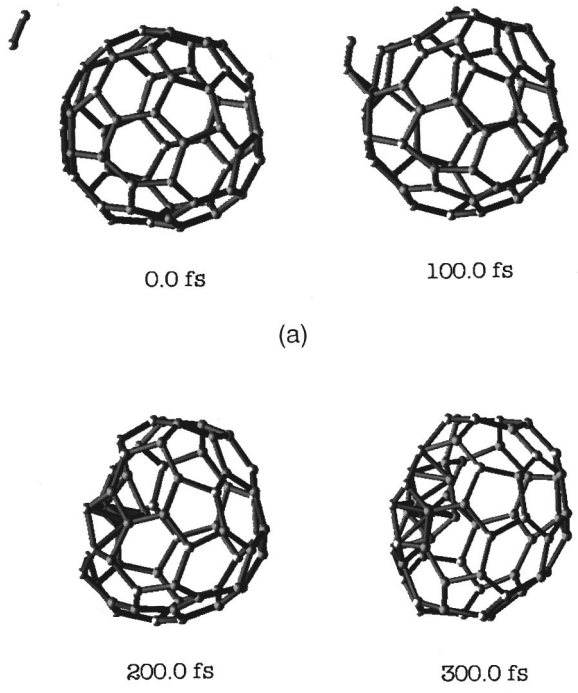

FIG. 2. (a) Initial configuration (0 fs) of ideal $C_{60}+C_2$, and the stable structure (100 fs) of the C_2-adsorbed C_{60} at 1000 K under the condition of quasistatic addition of C_2, in which kinetic energy of the incident C_2 is always kept below 2000 K. (b) Snapshots (at 200 and 300 fs) observed at 1000 K after removing the condition of quasistatic addition at 80 fs.

mentally be removed in an atmosphere. This simulation was performed at 7000 K assuming electronic ground state. We observed the similar reproducibility at 1000 K with Fermi distribution from the electronic states also.

In the reactivity simulations (C), we put a C_2 molecule outside a C_{60} with a distance, 4.0 Å, and set the system at $T=1000$ K. The incident C_2 had a tendency to increase its velocity during the reaction, since the reaction heat is equally partitioned to C_2 and C_{60}. Thus, C_2 may have a large velocity when it hits C_{60}, and the damage of C_{60} in this shock is generally not small.

In order to always achieve a good convergence of the electronic states at 1000 K, we applied an additional temperature control just for the incident C_2 molecule so as to keep its kinetic energy below 2000 K. Hereafter we call this the condition of quasistatic addition. Under this condition, C_2 was adsorbed vertically on a double bond of ideal C_{60} at 100 fs [Fig. 2(a)]. Since the electron affinity of C_2 is 3.3 eV (Ref. 27) and that of ideal C_{60} is 2.65 eV,[28] a charge transfer occurs from C_{60} to C_2. The reaction site at a double bond of C_{60} is therefore reasonable. We performed a similar simulation for the case of C_{2v} isomer of C_{60}. In this case, C_2 is adsorbed on the pentagon closer to the 6/6 bond bridging the fused pentagons at 1200 fs; see Fig. 3(a). The reaction site at the two fused pentagons is consistent with a theoretical conjecture[29] based on the Hückel picture. Dangling bonds exist outward from the carbon atoms violating IPR, and they are active with incident C_2. The present simulation reveals that the dangling bonds in the pentagons closer to the 6/6 bond bridging the fused pentagons are more active with respect to the C_2 addition compared to those in the other pentagons.

Note that these final structures are only stable at low temperatures. In fact, if we remove the condition of quasistatic addition before the reaction is completed (at 80 fs) and keep the temperature of the total system at 1000 K, we found a considerable deformation of the final structure of the ideal C_{60} adsorbed by C_2: The reaction proceeds strongly on the half sphere of C_{60}, and recombinations of bonds occurs on this side. On the opposite half sphere of C_{60}, the ideal cage structure is maintained; the structures at 200 and 300 fs are depicted in Fig. 2(b). The overall structures are somewhat similar to the optimized structure of C_{60} in the tunneling junction that was calculated recently by Joachim *et al.*[30] This reaction is not due to the initial velocity of C_2 (the kinetic energy of each carbon atom of C_2 at 80 fs corresponds to at most 2000 K only) but due to the interaction energy between C_2 and C_{60}.

On the contrary, in the case of C_{2v} isomer$+C_2$, the cage structure was destroyed also on the opposite half sphere of the C_{2v} isomer, and sp_2 character was lost almost everywhere; the structures at 200 and 300 fs are depicted in Fig. 3(b). In order to obtain a stable final structure, much longer simulation time would be required.

We also determined the most stable configuration of C_{60} with C_3 at 1000 K under the condition of the quasistatic addition. As a final structure, the C_3 forms a cross link on a hexagon of C_{60}, between the center of one double bond and the center of an opposite single bond of the hexagon; see Fig. 4. Note that the electron affinity of C_3 is 1.6 eV (Ref. 27) and charge transfer occurs from C_3 to the single bond of C_{60}, in contrast to the case of the C_2 addition.

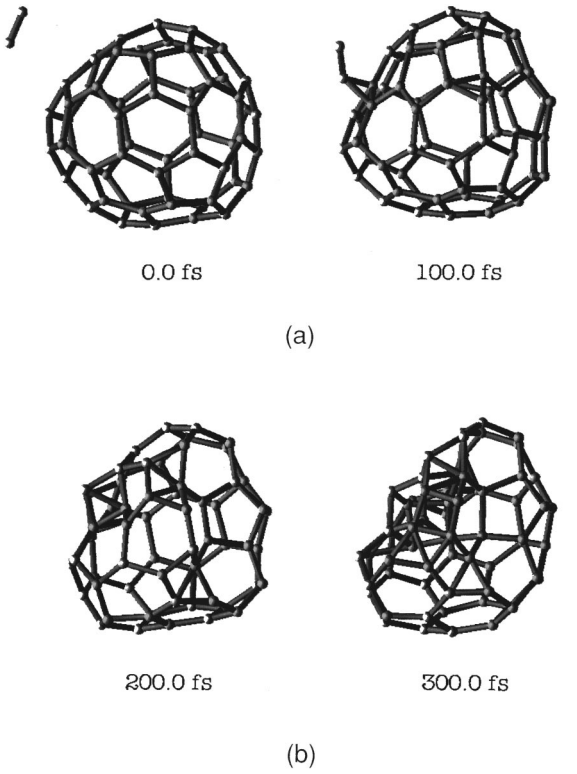

FIG. 3. (a) Initial configuration (0 fs) of C_{2v} isomer+C_2, and the stable structure (100 fs) of the C_2-adsorbed C_{2v} isomer at 1000 K under the condition of quasistatic addition of C_2. (b) Snapshots (at 200 and 300 fs) observed at 1000 K after removing the condition of quasistatic addition at 80 fs.

IV. SUMMARY

In summary, we have found that the finite temperature effect on the electronic states is important in order to discuss the stability and reactivity of fullerenes at finite temperatures, and to understand the formation processes. Only with the finite temperature effect on the electronic states could we estimate correctly the temperatures at which an ideal

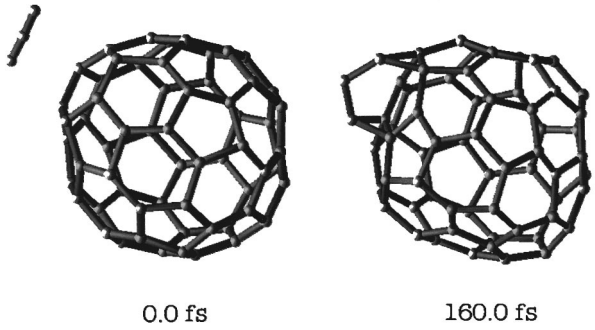

FIG. 4. Initial configuration (0 fs) of ideal C_{60}+C_3, and the stable structure (160 fs) of the C_3-adsorbed on ideal C_{60} at 1000 K under the condition of quasistatic addition of C_3.

C_{60} and its C_{2v} isomer (Fig. 1) become unstable. The estimated temperatures are much higher in ideal C_{60} (about 4500 K) than in the C_{2v} isomer (about 1500 K). Moreover, at 1000 K, we have found relatively strong reactivity of the C_{2v} isomer with C_2 compared to ideal C_{60}. At the same temperature, if we adopt the condition of quasistatic addition, we could find stable configuration of C_2 (or C_3) adsorbed C_{60}. Finally, we could regain C_{60} with almost I_h symmetry (not its C_{2v} isomer, although there was an equal possibility) by injecting C_2 to the hole of a C_{58} molecule, which was constructed from an ideal C_{60} by subtracting C_2 and relaxing. These results offer evidence of IPR in the late stage of the formation process of C_{60}.

ACKNOWLEDGMENTS

This research has been supported in part by a grant-in-aid program of the respected area ''carbon clusters'' by the Ministry of Education, Science and Culture of Japan. The authors would like to thank Professor Eiji Osawa for encouraging discussions and Dr. Keivan Esfarjani for many helpful discussions. They are also grateful to the Materials Information Science Group of the Institute for Materials Research, Tohoku University, for their continuous support of the supercomputing facilities.

[1] H. Kroto, J. R. Heath, S. C. O'Brien, R. F. Curl, and R. E. Smalley, Nature **318**, 162 (1985).
[2] R. E. Haufler, J. Conceicao, L. P. F. Chibante Y. Chai, N. E. Byrne, S. Flanagan, M. M. Haley, S. C. O'Brien, C. Pan, Z. Xiao, W. E. Billups, M. A. Ciufolini, R. H. Hauge, J. L. Margrave, L. J. Wilson, R. F. Curl, and R. E. Smalley, J. Phys. Chem. **94**, 8634 (1990); see also Ref. 4.
[3] H. W. Kroto, Nature **329**, 529 (1987).
[4] A. J. Stone and D. J. Wales, Chem. Phys. Lett. **128**, 501 (1986); see aslo Ref. 22.
[5] T. Wakabayashi and Y. Achiba, Chem. Phys. Lett. **190**, 465 (1992).
[6] D. H. Robertson, D. W. Brenner, and C. T. White, J. Phys. Chem. **96**, 6133 (1992).
[7] G. v. Helden, N. G. Gotts, and M. T. Bowers, Nature **363**, 60 (1993).
[8] J. M. Hunter, J. L. Fye, E. J. Rockamp, and M. F. Jarrold, J. Phys. Chem. **98**, 1810 (1994).
[9] M. Fujita, Fullerene Sci. Technol. **1**, 365 (1993).
[10] R. L. Murry, D. L. Strout, G. K. Odom, and G. E. Scuseria, Nature **366**, 665 (1993).
[11] S. Serra, S. Sanguinetti, and L. Colombo, J. Chem. Phys. **102**, 2151 (1995).
[12] J. R. Chelikowsky, Phys. Rev. Lett. **67**, 2970 (1991); Phys. Rev. B **45**, 12 062 (1992).
[13] C. Xu and G. E. Scuseria, Phys. Rev. Lett. **72**, 669 (1994).
[14] G. Galli and F. Mauri, Phys. Rev. Lett. **73**, 3471 (1994).
[15] R. Car and M. Parrinello, Phys. Rev. Lett. **55**, 2471 (1985).
[16] M. C. Payne, M. Needels, and J. D. Joannopoulos, Phys. Rev. B **37**, 8138 (1988).
[17] A. Alavi, J. Kohanoff, M. Parrinello, and D. Frenkel, Phys. Rev. Lett. **73**, 2599 (1994).
[18] Q. M. Zhang, J. Y. Yi, and J. Bernhole, Phys. Rev. Lett. **66**, 2633 (1991).
[19] B. P. Feuston, W. Andreoni, M. Parrinello, and E. Clementi, Phys. Rev. B **44**, 4056 (1991).

[20] G. B. Adams, J. B. Page, O. F. Senkey, K. Sinha, J. Menendez, and D. R. Huffmann, Phys. Rev. B **44**, 4502 (1991).
[21] Y. Maruyama, H. Kamiyama, K. Ohno, and Y. Kawazoe, Science Report RITU (Tohoku Univ.) **A-39**, 15 (1993); in *Advanced Materials '93 I/B: Magnetic, Fullerene, Dielectric, Ferroelectric, Diamond, and Related Materials*, edited by M. Homma *et al.* (Elsevier, Amsterdam, 1994), p. 1215.
[22] K. Raghavachari and C. M. Rohlfing, J. Phys. Chem. **96**, 2463 (1992).
[23] N. D. Mermin, Phys. Rev. **137**, A1441 (1965).
[24] O. Gunnarsson and B. I. Lundqvist, Phys. Rev. B **13**, 4274 (1976).
[25] N. Troullier and J. L. Martins, Phys. Rev. B **46**, 1754 (1992).
[26] B.-L. Gu, Y. Maruyama, J.-Z. Yu, K. Ohno, and Y. Kawazoe, Phys. Rev. B **49**, 16 202 (1994).
[27] S. Yang, K. J. Taylor, M. J. Craycraft, J. Conceicao, C. L. Pettiette, O. Cheshnovsky, and R. E. Smalley, Chem. Phys. Lett. **144**, 431 (1988).
[28] S. H. Yang, C. L. Pettiette, J. Conceicao, O. Cheshnovsky, and R. E. Smalley, Chem. Phys. Lett. **139**, 233 (1987); R. L. Hettich, R. N. Compton, and R. H. Ritchie, Phys. Rev. Lett. **67**, 1242 (1991).
[29] J. Aihara and S. Takata, J. Chem. Soc. Perkin Trans. **2**, 65 (1994).
[30] C. Joachim, J. K. Gimzewski, R. R. Schlittler, and C. Chavy, Phys. Rev. Lett. **74**, 2102 (1995).